TRITA-PFU-78-06

ON THE BALANCE OF A LINEAR PLASMA COLUMN CONFINED IN A TRANSVERSE MAGNETIC FIELD

B. Lehnert

Stockholm, August 1978

Department of Plasma Physics and Fusion Research
Royal Institute of Technology
S-100 44 Stockholm 70, Sweden

ON THE BALANCE OF A LINEAR PLASMA COLUMN CONFINED IN A TRANSVERSE MAGNETIC FIELD

B. Lehnert
Royal Institute of Technology, S-10044 Stockholm 70,Sweden

ABSTRACT

The equilibrium features are investigated of a straight plasma column being confined in a purely transverse magnetic field, part of which is being generated by external conductors. Provided that stability can be secured at high beta values, the reduced transport of particles and heat in the axial direction should allow for large axial temperature gradients. It is then expected that temperatures even leading to ignition can be achieved in a pure plasma, at technically realistic column lengths.

1. Introduction

In an ideal magnetic bottle the guiding centre orbits form closed paths both in the directions along and across the magnetic field. At least in principle, such a bottle can be realized by closed toroidal schemes with a main poloidal field. The complexity of toroidal geometry can in two ways be diminished at the expense of a reduced confinement. The first is represented by open bottles, such as mirror devices, where the transverse guiding-centre motion still forms closed orbits, but particles are lost along the field lines. The second way is represented by all straight or sector geometries in which the magnetic field lines are closed within the confinement volume, but where the guiding-centre motions across the field lines lead out to surrounding vessel walls. This second type of schemes includes ordinary and hardcore pinches without an axial magnetic field, as well as straight "Extrap" devices [1-3] of which one type is outlined in Fig.1. The present context is restricted to an analysis of the plasma balance in a stable state of such devices. Some comments on stability are made later in this paper.

The confinement of a straight plasma column by a purely transverse magnetic field does not only represent a first step towards completely closed toroidal geometry, but also has some merits of its own. Thus, in a strong magnetic field the end losses by transverse guiding-centre motions should become much smaller than the end losses in mirror machines at least in certain parameter ranges such as in the case of a high plasma density. Since the field lines do not intersect the end electrodes in a pinch configuration of the present type, the heat and particle transport to these electrodes also becomes much smaller than in straight pinches being stabilized by an axial magnetic field. In other words, the reduced axial transport in straight Extrap geometry and similar schemes should allow for axial temperature gradients and high temperatures within certain parts of the plasma column. Further, steady confinement should become possible at high beta values, by feeding strong d.c. currents between the end electrodes. Such an arrangement

also has the merits of low complexity from the technological point of view.

2. Starting Points of Analysis on Equilibrium State

The build-up of a fully ionized plasma column from a mass of neutral gas becomes relatively simple in straight geometry, because large amounts of power can be imposed by an electrode discharge. Especially when the magnetic vacuum field has a zero line at the axis of the plasma column, such as in Fig.1, a pinched plasma is expected to build up radially outwards from this line [3,4]. Preliminary experimental results seem to confirm this behaviour [5].

Assuming a steady state to be reached, and with plasma stability being accepted as a working hypothesis, the particle, momentum, and heat balance of a steady equilibrium as well as its build-up phase have earlier been considered to some detail for toroidal geometry [1-3,6]. Here we concentrate on straight Extrap and similar geoemtries, part of the features of which have already been considered in connection with the toroidal sector case [3].

2.1. General Assumptions

The analysis of the coming sections is based on the following general assumptions:

(i) All field quantities are time-independent.

(ii) The plasma is quasi-neutral, with n standing for the ion and electron particle densities.

(iii) The density n is large enough for the plasma to become "impermeable" to neutral gas. Thus, narrow partially ionized boundary regions are created, both in the form of a cold-mantle surrounding the cylindrical surface of the plasma column in the xy plane of Fig. 1, and in the form of layers at the electrode surfaces bounding the plasma column in the axial z direction. Only the balance of the fully ionized part of the plasma body will be treated more

in detail, whereas a short discussion on plasma-neutral gas interaction is postponed to Sections 2.3 (iii) and 4.4.

(iv) The Nernst effects [7-9] are neglected in the present simplified treatment.

(v) The axial length L of the plasma column is much larger than the average radius $\bar{a}$ of its cross section.

(vi) At the pinch axis there is a weak-field region, the radial extension of which becomes comparable to or smaller than the local electron Larmor radius. This region is excluded from the present macroscopic analysis. It could, in principle, give rise to enhanced axial losses but is not expected to be of crucial importance at strong discharge currents J and large axial lengths L of the plasma column.

(vii) The inertia forces due to a macroscopic flow of the plasma are neglected. This is usually a good approximation when the fluid velocity remains much smaller than the thermal velocity of ions.

2.2. Basic Equations

Due to the antiparallel axial drift motions of ions and electrons in a system of finite axial length, it is necessary to distinguish between the ion and electron temperatures T_i and T_e. We therefore adopt macroscopic two-fluid equations of the simplified form (compare Ref. [10])

$$\mathrm{div}(n\underline{v}_i) = \mathrm{div}(n\underline{v}_e) = 0 \tag{1}$$

$$0 = en(\underline{E} + \underline{v}_i \times \underline{B}) - \nabla p_i - e^2 n^2 \eta (\underline{v}_i - \underline{v}_e) \tag{2}$$

$$0 = -en(\underline{E} + \underline{v}_e \times \underline{B}) - \nabla p_e + e^2 n^2 \eta (\underline{v}_i - \underline{v}_e) \tag{3}$$

$$\frac{3}{2}\,\mathrm{div}(p_i \underline{v}_i) + p_i\,\mathrm{div}\,\underline{v}_i =$$

$$= 3e^2n^2\eta(k/m_i)(T_e - T_i) - \mathrm{div}\,\underline{q}_i + \Pi_t \qquad (4)$$

$$\frac{3}{2}\,\mathrm{div}(p_e \underline{v}_e) + p_e\,\mathrm{div}\,\underline{v}_e =$$

$$= -3e^2n^2\eta(k/m_i)(T_e - T_i) - \mathrm{div}\,\underline{q}_e + \eta j^2 - \Pi_r \qquad (5)$$

Here SI-units are applied, $\underline{v}_i$, $\underline{v}_e$ are the fluid velocities of ions and electrons, $\underline{E}$ and $\underline{B}$ the electric and magnetic fields, $p_i = nkT_i$, $p_e = nkT_e$, $\underline{q}_i$, $\underline{q}_e$ the heat flow vectors, and $\underline{j}$ the current density. Further, with ν_{ei} and ν_{ii} as the electron-ion and ion-ion collision frequencies, the resistivity $\eta = m_e\nu_{ei}/e^2n$ has the value $\eta_\perp = k_\eta/T_e^{3/2}$ across $\underline{B}$ with $k_\eta = 129\ (\ell n\Lambda)$ [11], and the ion heat conductivity becomes $\underline{q}_i = \underline{q}_{i_\perp} = -\lambda^* \underline{\nabla}_\perp T_i$ across $\underline{B}$ with $\lambda^* = 5nk^2T_i m_i \nu_{ii}/e^2B^2 = k_2 n^2\sqrt{A}(\ell n\Lambda)/B^2\sqrt{T_i}$ and $k_2 \simeq 1.5 \times 10^{-42}$. Finally

$$\Pi_t = f_\alpha k_t n^2 \rho_t \qquad (6)$$

is the thermonuclear reaction power being shared by charged constituents where $f_\alpha \simeq 0.2$, $k_t \simeq 7.05 \times 10^{-13}$ joules for the DT-reaction, ρ_t is the corresponding reaction rate [12], and

$$\Pi_r = k_{rb} n^2\sqrt{T_e} + k_{rc} n B^2 T_e \qquad (7)$$

is the loss due to bremsstrahlung and unabsorbed cyclotron radiation with $k_{rb} \simeq 1.7 \times 10^{-40}$, $k_{rc} \simeq 8 \times 10^{-24}$ [13], $Z = 1$ throughout this paper, and the rest of the symbols have their

conventional meaning.

With $m = m_i + m_e$, the substitutions

$$\underline{v}_i = \underline{v} + (m_e/enm)\underline{j} \qquad \underline{v}_e = \underline{v} - (m_i/enm)\underline{j} \tag{8}$$

and $p = p_i + p_e$, eqs. (1)-(5) are combined to

$$\mathrm{div}(n\underline{v}) = 0 \tag{9}$$

$$\mathrm{div}\ \underline{j} = 0 \tag{10}$$

$$\underline{j} \times \underline{B} = \nabla p \tag{11}$$

$$n\underline{j} = \underline{E} + \underline{v} \times \underline{B} - (1/enm)(m_i \nabla p_i - m_e \nabla p_e) \tag{12}$$

$$\frac{3}{2}\,\mathrm{div}(p\underline{v}) + p\,\mathrm{div}\,\underline{v} - (3/2em)\,\mathrm{div}\left[(m_i p_e - m_e p_i)\underline{j}/n\right] -$$

$$- (m_i p_e - m_e p_i)\,\mathrm{div}(\underline{j}/emn) =$$

$$= n\underline{j}^2 - \mathrm{div}(\underline{q}_i + \underline{q}_e) + \Pi_t - \Pi_r \tag{13}$$

2.3. Parameter Ranges and Approximations

We introduce $\bar{a}$ and $\bar{j}$ as the average pinch radius and current density within the plasma cross section which is traversed by the total current $J = \pi \bar{a}^2 \bar{j}$. We also define the beta value

$$\beta = 8kn_o(T_{io} + T_{eo})/\mu_o(\bar{a}\,\bar{j})^2 \qquad (14)$$

where subscript ($_o$) refers to the pinch axis. A first approximation of the radial balance of forces in eq. (11) corresponds to $\beta \approx 1$. In this paper the deductions are restricted to values of β being of order unity, and to parameter ranges being roughly given by

$$\left.\begin{array}{ll} \bar{a} \approx 10^{-2} & \text{m} \\ 3 \times 10^4 \lesssim J \lesssim 3 \times 10^6 & \text{A} \\ 3 \times 10^5 \lesssim T_{io},\ T_{eo} \lesssim 10^8 & \text{K} \\ 10^8 \lesssim \bar{j} \lesssim 10^{10} & \text{A/m}^2 \\ 3 \times 10^{21} \lesssim n_o \lesssim 3 \times 10^{23} & \text{m}^{-3} \end{array}\right\} \qquad (15)$$

With these ranges the following estimations are now made:

(i) Heat conduction across $\underline{B}$ is mainly due to the ions. The ratio between this loss and the ohmic heating power is of the order (see also Ref. [3])

$$\Lambda = |\mathrm{div}\underline{q}_i|/\eta j^2 \approx 5\beta^2 m_i \nu_{ii}/256 m_e \nu_{ei} = 0.48\beta^2\sqrt{A} \qquad (16)$$

If the plasma is bounded by a vacuum boundary, heat conduction would tend to establish a uniform temperature over the plasma cross section. In presence of a partially ionized

boundary layer, the plasma temperature would on the other hand be kept at a low value, of the order of $T_b \simeq 5 \times 10^4$K, at the inner "interface" of this layer. From eq. (16) is seen that the corresponding heat conduction loss from the hot plasma core would then be of the same order of magnitude as the ohmic heat production. Here we restrict ourselves to values of β and A for which $\Lambda < 1$ and there is a net heating power from ηj^2 - div $\underline{q}_i$. Since Λ of eq. (16) is independent of the parameters $\bar{a}$, J, T_i, T_e, n we shall treat this ratio as a constant in the first approximation.

(ii) From expression (7) is easily seen that the radiation loss Π_r can be neglected compared to ηj^2 within the lower parts of the parameter ranges given by expression (15), but not within the upper parts of the same ranges.

(iii) The penetration length of fast neutral particles becomes $L_{nf} = 1/n\sigma_{cf}$ where $1/\sigma_{cf} \simeq 5 \times 10^{18}$ m^2 at plasma temperatures exceeding $T_b \simeq 5 \times 10^4$K [14]. The corresponding impermeability condition $n_o \bar{a} \gg 1/\sigma_{cf}$ is seen to be satisfied within the parameter ranges (15). In particular, with n_{na} as the neutral gas density n_n at a boundary of the plasma and the coordinate ζ being perpendicular to the boundary and pointing into the plasma body, the local distribution of neutrals becomes

$$n_n = n_{na} \exp(-n\sigma_{cf}\zeta) \tag{17}$$

The influence of the neutral gas on the heat balance can then be estimated by subtracting a term

$$\Pi_n = n n_n \left[e\phi_i \zeta + \tfrac{3}{2} k(\rho_{in} T_i + \rho_{en} T_e) \right] \equiv n n_n Q_n \tag{18}$$

from the right-hand member of eq. (13). Here ϕ_i stands for the ionization potential, ξ for the ionization rate, and ρ_{in}, ρ_{en} for the reaction rates of ions and electrons due to all other impacts with the neutrals than those leading to ionization. The influence of Π_n can be estimated by comparing it with the ohmic heating power in terms of the ratio $\vartheta = \Pi_n/\eta j^2 = \theta(\zeta)$. In particular, for $\zeta = \bar{a}$, it is then easily seen that $\theta(\bar{a}) << 1$ in the parameter ranges (15). Thus, for these ranges the heat balance in the hot plasma core should hardly be affected by neutral gas interaction. On the other hand, neutral gas interaction should have an influence in the end electrode layers, to which we will return later in this paper.

3. Particle and Momentum Balance

We now turn to the mass flow, the electric currents, and the particle drift motions as described by eqs. (1)-(3) and (8)-(12).

3.1. The Pattern of the Electric Current Density

In the special case of a plasma column of circular symmetry in a cylindrical frame $(r\varphi z)$, the current density and the magnetic field would have the forms $\underline{j} = (j_r, o, j_z)$ and $\underline{B} = (0, B, 0)$ when the plasma cross section is assumed to vary in thickness in the axial z direction. From the curl of eq. (11) it is seen, however, that $\partial B_\varphi / \partial z = 0$ and $j_r = 0$, i.e. $\underline{j} = [0, 0, j_z(r)]$ and the plasma column has to be uniform in the axial direction.

In the more general case of a non-circular plasma cross section, the balance equations are also satisfied by $j_x = 0$, $j_y = 0$, $B_z = 0$ in the frame (xyz) of Fig.1. Throughout this paper we therefore restrict ourselves to columns of uniform cross section in the axial direction. As a consequence, eq. (11) yields

$$\underline{j} \cdot \underline{\nabla} p = 0 \; ; \qquad \frac{\partial}{\partial z} \left[n(T_i + T_e) \right] = 0 \tag{19}$$

3.2. Variations in the Direction along the Magnetic Field

The case of the previous section yields $\underline{j} \cdot \underline{B} = 0$. From eq. (11) we further have $\underline{B} \cdot \underline{\nabla} p = 0$. Within the parameter range of interest in this connection, the assumption of a constant electric potential along $\underline{B}$ should become a valid approximation. Eqs. (2) and (3) then yield $\underline{B} \cdot \underline{\nabla} p_i = 0$ and $\underline{B} \cdot \underline{\nabla} p_e = 0$. If, in addition, the thermal conductivity due to the electron motion along $\underline{B}$ is high enough for $\underline{B} \cdot \underline{\nabla} T_e \simeq 0$, we also have $\underline{B} \cdot \underline{\nabla} n \simeq 0$ and $\underline{B} \cdot \underline{\nabla} T_i \simeq 0$.

It is finally observed that there are no accelerating forces of the ion and electron fluid motions along $\underline{B}$ in eqs. (2) and (3). Consequently, we can put $\underline{B} \cdot \underline{v}_i = 0$ and $\underline{B} \cdot \underline{v}_e = 0$.

When using the symbols $\underline{v}_i$, $\underline{v}_e$, $\underline{v}$, $\underline{j}$, and $\underline{\nabla}$ in the coming sections, it should therefore be kept in mind that they refer to the directions being perpendicular to $\underline{B}$ only.

3.3. Fluid and Guiding Centre Motions

From eqs. (2), (3) and (11) we now obtain

$$\underline{v}_i = \underline{E} \times \underline{B}/B^2 + (\underline{B}/enB^2) \times \underline{\nabla}p_i - (n/B^2)\underline{\nabla}p \tag{20}$$

$$\underline{v}_e = \underline{E} \times \underline{B}/B^2 - (\underline{B}/enB^2) \times \underline{\nabla}p_e - (n/B^2)\underline{\nabla}p \tag{21}$$

which can be combined with eq. (12) to

$$\underline{v}_i = \underline{v} + (m_e\underline{B}/enmB^2) \times \underline{\nabla}p \tag{22}$$

$$\underline{v}_e = \underline{v} - (m_i\underline{B}/enmB^2) \times \underline{\nabla}p \tag{23}$$

as is also obvious from eqs. (11) and (8). Concerning the fluid velocity $\underline{v}$ of the centre-of-mass motion, the following features should be observed:

(i) The transverse components v_x, v_y vanish when the Nernst effect is neglected. Then there is no flux of matter from the fully ionized plasma core towards the "interface" of the partially ionized layer which is situated at the cylindrical surface bounding the plasma column. In the case $T_i = T_e$ this also implies that the outward directed

diffusion across $\underline{B}$ due to finite resistivity η is cancelled by the inward directed drift motion due to the axial electric field $E_z = \eta j_z$ in eq. (12).

(ii) Eqs. (1)-(13) allow, in principle, for an un-accelerated axial mass motion $\underline{v} = (0,0,v_z)$. However, there are reasons to assume this motion to be negligible, because the ions entering the plasma column are formed from neutral particles of low temperature in the anode region and are starting there in cycloid-like orbits at the time of creation. Provided that there is no excessively large electric field within this region, it is therefore justified to assume the corresponding initial value of v_z to be small. In addition, eq. (9) yields $\partial(nv_z)/\partial z = 0$ and $\partial n/\partial z = 0$ for $v_z = \text{const.} = 0$. In combination with eq. (19) this would lead to the singular case $\partial(T_i + T_e)/\partial z = 0$ which has no physical interest in this connection. Therefore we have to put $v_z = 0$.

We finally consider the fluxes of ions and electrons in the case $\underline{v} = 0$, as given by eqs. (22) and (23) which yield

$$\operatorname{div}(n\underline{v}_i) = (m_e/em)\underline{u}_B \cdot \underline{\nabla}p = -(m_e/m_i)\operatorname{div}(n\underline{v}_e) \qquad (24)$$

where

$$\underline{u}_B = (2\underline{B}/B^3) \times \underline{\nabla}B + (1/B^2)\operatorname{curl} \underline{B} \qquad (25)$$

The quantity $\underline{u}_B$ demonstrates the relationship between fluid and orbit theory. It includes the contributions to the guiding centre drift from the inhomogeneity of $|\underline{B}|$ and from the curvature of the magnetic field lines. The guiding centre drifts do not only produce a translation of the charged particles but

can also give rise to compression or expansion of the ion and electron fluids. All these effects are taken care of in the macroscopic fluid theory and need not be discussed further in detail. It should only be observed that the axial losses of particles in the case $\underline{v} = 0$ are given by the current density $\underline{j}$ only, as shown by eqs. (22), (23), (8) and expected from simple physical reasons.

4. Heat Balance

The heat balance of a system having finite axial dimensions has earlier been discussed in connection with Extrap sector geometry [3]. Here we make a first crude approach to the case of straight geometry by treating the ratio Λ of Section 2.3(i) as a constant.

4.1. General Equations of Fully Ionized Plasma

With the present assumptions and starting points eq. (19) can be used to rewrite the left-hand members of eqs. (4) and (5) yielding

$$[m_e kj/em(T_i + T_e)]\cdot[(\tfrac{5}{2} T_i + \tfrac{3}{2} T_e)\frac{\partial T_i}{\partial z} + T_i \frac{\partial T_e}{\partial z}] =$$

$$= 3e^2 n^2 \eta (k/m_i)(T_e - T_i) - \Lambda \eta j^2 + \Pi_t \qquad (26)$$

$$- [m_i kj/em(T_i + T_e)]\cdot[T_e \frac{\partial T_i}{\partial z} + (\tfrac{3}{2} T_i + \tfrac{5}{2} T_e) \frac{\partial T_e}{\partial z}] =$$

$$= - 3e^2 n^2 \eta (k/m_i)(T_e - T_i) + \eta j^2 - \Pi_r \qquad (27)$$

Here the condition $v_z = 0$ makes the ions move much more slowly from the anode side into the plasma column than the electrons are moving in the opposite direction from the cathode side. This accounts for the factors m_e/m and $-m_i/m$ in front of the left-hand members. Further, the terms including $\partial T_e/\partial z$ and $\partial T_i/dz$ in eqs. (26) and (27) are due to the compression works $p_i \mathrm{div} \underline{v}_i$ and $p_e \mathrm{div} \underline{v}_e$, respectively. These terms give contributions to the heat balance in addition to those from the axial fluxes of particle energy being represented by $(3/2)\mathrm{div}(p_i \underline{v}_i)$ and $(3/2)\mathrm{div}(p_e \underline{v}_e)$.

It is of special interest to study eqs. (26) and (27) in the internal hot regions of the plasma cross section, i.e. at fixed x and y in Fig.1. In this case all quantities become functions of z only. We also assume a nearly uniform current density, i.e. $j \simeq \bar{j}$. Solving then for dT_i/dz and dT_e/dz and dropping subscript $(_o)$ in the definition (14) of beta, these equations can be rearranged to the forms

$$C \frac{dT_i}{dz} = \left[\frac{3}{2} T_i + \frac{5}{2} T_e - (m_e/m_i) T_i\right](T_e - T_i) +$$

$$+ \left(\frac{3}{2} T_i + \frac{5}{2} T_e\right) U + (m_e/m_i) T_i W \qquad (28)$$

$$- C \frac{dT_e}{dz} = \left[T_e - (m_e/m_i)\left(\frac{5}{2} T_i + \frac{3}{2} T_e\right)\right](T_e - T_i) +$$

$$+ T_e U + (m_e/m_i)\left(\frac{5}{2} T_i + \frac{3}{2} T_e\right) W \qquad (29)$$

where

$$C = 80\, m_i m_e k^2 (T_i + T_e)^3 T_e^{3/2} / \mu_o^2 m_e^3 k_\eta \beta^2 \bar{a}^4 j^3 \qquad (30)$$

$$U = m_i (\Pi_t - \Lambda \eta j^2) / 3e^2 k \eta n^2 \qquad (31)$$

$$W = m_i (\eta j^2 - \Pi_r) / 3e^2 k \eta n^2 \qquad (32)$$

Concerning the boundary conditions of eqs. (28) and (29) the following points should be observed:

(i) The anode is assumed to be located at $z = 0$ and the cathode at $z = z_a + L + z_c$. Near the anode and cathode, i.e. in the regions $0 < z < z_a$ and $z_a + L < z < z_a + L + z_c$ there are partially ionized layers of small thickness z_a and z_c as compared to the column length L. The condition $v_z = 0$ implies that the ions are moving slowly in the positive z direction and the electrons rapidly in the negative z direction.

(ii) The electrons are created in the cathode region and leave the cathode layer at a temperature $T_b \approx 5 \times 10^4$ K.

(iii) When moving in the negative z direction, the electrons are being subject to ohmic heating. Due to the slow ion motion, and provided that this heating becomes larger than the rate of heat loss, we expect the electrons to become hotter and T to be larger when moving away from the cathode in the negative z direction. The ions are almost static and nearly adopt the local electron temperature.

(iv) The ions are created in the anode region and leave the interface $z = z_a$ between the anode layer and the fully ionized plasma at a temperature $T_i(z_a) \approx T_b$. When entering the fully ionized plasma region, they meet the hot counter-streaming electrons and are rapidly heated to a temperature being close to that of the electrons. Consequently, under general conditions the ion and electron temperatures can differ appreciably within a narrow anode region of thickness z_a which extends from the plane $z = 0$ in the positive z direction. The highest ion temperature is expected to arise near the "interface" $z = z_a$ between this region and the main part of the plasma column within which usually $T_i \approx T_e$. Further modifications of the temperature distributions near the electrode surfaces arise from neutral gas interaction, as discussed later in Section 4.4.

4.2. Limiting Case of Equal Ion and Electron Temperatures

In the limiting case $T_i = T_e \equiv T$ of very strong coupling between ions and electrons, the sum of eqs. (26) and (27) yields

$$- \left[5(m_i - m_e)kj/2em\right] \frac{dT}{dz} = (1 - A)\eta j^2 + \Pi_t - \Pi_r \tag{33}$$

which relation is also obtained from eq. (13) in combination with eq. (19). Eq. (33) can be integrated to

$$L \cdot j = \frac{5k(m_i - m_e)}{2ek_\eta m} \int_{T_b}^{T(z_a)} \frac{T^{3/2}\, dT}{1 - A + c_t(\rho_t/\sqrt{T}) - C_r} \tag{34}$$

where

$$c_t = \mu_0^2 b^2 J^2 f_\alpha k_t / 256\pi^2 k^2 k = f_\alpha k_t C_r / k_{rb} \tag{35}$$

In eq. (34) cyclotron radiation has been neglected for three reasons. First, it becomes comparable to the bremsstrahlung loss only at the highest temperature within the ranges (15). Second, the magnetic field becomes relatively weak within the hot parts of the plasma near the axis. Third, cyclotron radiation can be reflected by surrounding metal walls and reabsorbed in the plasma. The relation between $L \cdot j$ and T of eq. (34) simply expresses the balance between the net heat production and the end losses from the plasma column. Two special cases are of interest here:

(i) In an ohmically heated plasma with negligible thermonuclear power and bremsstrahlung

$$T(z) = \left[T_b^{5/2} + (1 - \Lambda) T_\eta^{5/2} (1 - z/L)\right]^{2/5} \tag{36}$$

where

$$T_\eta = \left[e k_\eta m L j / (m_i - m_e) k\right]^{2/5} \tag{37}$$

With $T_b \ll T_\eta$ a maximum temperature $T(z = z_a) \approx T_\eta (1-\Lambda)^{2/5}$ is obtained.

(ii) In a plasma being mainly heated by thermonuclear reactions, the term containing c_t dominates at high temperatures of the integral in eq. (34). Here thermonuclear temperatures can be reached at smaller values of Lj than in absence of alpha particle heating.

4.3. Limiting Case of Negligible Ion Current

With the condition $v_z = 0$ and $m_e \ll m_i$ the ion current can be neglected and the left-hand member of eq. (26) be put equal to zero with good approximation. Consequently, eqs. (26) and (27) reduce to

$$T_i - T_e = (m_i f_\alpha k_t \rho_t T_i^{3/2} / 3e^2 k k_\eta) - (\Lambda m_i j^2 / 3e^2 k n^2) \tag{38}$$

$$- \left[kj/e(T_i + T_e)\right] \cdot \left[T_e \frac{dT_i}{dz} + \left(\frac{3}{2} T_i + \frac{5}{2} T_e\right) \frac{dT_e}{dz}\right] =$$

$$= (1 - \Lambda) \eta j^2 + \Pi_t - \Pi_r \tag{39}$$

Combination of eqs. (38) and (39) then leads to one first-order differential equation for each of the dependent variables, i.e. T_i or T_e. In the fully ionized plasma region being described by the system of eqs. (38) and (39) the boundary conditions of T_i and T_e can then no longer be chosen independently of each other.

The relative deviation $|T_i-T_e|/(T_i+T_e)$ from equal ion and electron temperatures can be estimated from eq. (38). When this deviation becomes small, the solution of eqs. (38) and (39) approaches the limit given by eqs. (33)-(35). We finally notice that there is one solution of equation (38) leading to the singular case $T_e \neq 0$ in the limit $T_i = 0$. This solution is excluded from the present analysis.

4.4. The Partially Ionized Electrode Layers

In the electrode layers we neglect Π_t and Π_r, use the approximation $T_i = T_e = T$, and combine the results of Sections 2.3(iii) and 4.2. At the anode we then have

$$\frac{dT}{dz} = \left[2em/5(m_i - m_e)kj\right] \cdot \left[nn_{na}Q_n\exp(-n\sigma_{cf}z) - (1-A)nj^2\right] \quad (40)$$

Within the present parameter ranges it can be seen that Π_n becomes larger than nj^2 at small distances from the plane $z = 0$. This implies that T increases here when moving away from the anode. The conditions are analogous in the cathode layer.

The presence of neutral gas in the electrode layers therefore keeps the plasma temperature at low values in the regions being close to the electrode surfaces. In this connection it should be investigated whether the plasma-electrode interaction can be reduced by terminating the straight pinch configuration by "end vessels" containing the electrodes, and where at least the partially ionized plasma can have a larger geometrical cross section than that of the fully ionized column.

5. Numerical Examples

The obtained results are now illustrated by some numerical examples, with applications both to laboratory investigations on modest scale and to a possible ignition experiment.

5.1. Equal Ion and Electron Temperatures

We first turn to the limit of equal ion and electron temperatures represented by eqs. (33)-(37):

(i) The case of pure ohmic heating is demonstrated by the characteristic temperature T as given by Fig.2. It is expected from the figure and from eq. (36) that comparatively high temperatures can be reached within a considerable fraction of the plasma column length, even in devices of modest scale.

(ii) The case of a subsidiary heating by thermonuclear reactions is demonstrated by Fig.3 where $J = 2.5 \times 10^6 A$, $\bar{a} = 10^{-2} m$, $\beta = 0.5$, and a mean value $A = 2.5$ has been introduced for a deuterium-tritium mixture. The figure indicates that alpha particle heating becomes important at temperatures T above some $2 \times 10^7 K$. To reach this temperature, the plasma column should have a length of about 30 m, with a steady-state potential drop of about 3 kV between the electrodes. The alpha particle heating power would then become about 100 MW/m. These data predict a pulsed ignition experiment to become realizable, provided that the plasma remains stable during the pulse time and that the electrode regions do not introduce impurities which lower the plasma temperature substantially. The current density in such an experiment becomes appreciable, i.e. $j \approx 8 \times 10^9 A/m^2$, and it would have to be imposed at ion densities of the order of $n = 10^{23} m^{-3}$. Finally, with the present data, the Larmor radius of alpha particles at the plasma boundary becomes somewhat smaller than $\bar{a}$. Thus, at least a substantial fraction of these particles should be contained and thermalized within the plasma.

5.2. Unequal Ion and Electron Temperatures

There are, in principle, two mechanisms which give rise to a difference between the ion and electron temperatures in the present system. The first is due to an unbalance between the local heat sources and sinks. This mechanism is present also when the ion current can be neglected, as in the case of eqs. (38) and (39). The second mechanism originates from the convective axial motion of the charged particles in presence of axial temperature gradients. This produces large temperature gradients close to the anode, as described earlier in Section 4.1 (iv) for the case of a small but finite ion current.

5.2.1. Balance in Absence of Ion Currents

The case of negligible ion currents is now illustrated by two examples with $\bar{a} = 10^{-2}$m and $\beta = 0.5$ for which the solutions of eq. (38) have been plotted in Fig.4.

(i) In a small laboratory experiment with $J = 6 \times 10^4$A, the quantity $\theta_{ei} \equiv [(T_e/T_i)-1]$ varies with T_i as shown by curve (a) in the figure. Here the limit $T_i \approx T_e$ of Section 4.2 becomes a rather good approximation at temperatures $T_i < 10^6$K.

(ii) In an "ignition experiment" with $A = 2.5$ and $J = 2.5 \times 10^6$A, the behaviour of θ_{ie} becomes as shown by curve (b). Here θ_{ie} is very small and positive up to $T_i \approx 2 \times 10^7$K, but drops steeply to negative values at higher temperatures where there is a dominating alpha particle heating.

5.2.2. Balance in Presence of Ion Currents

The behaviour of an ohmically heated plasma in which Π_t and Π_r are neglected but ion current effects are being taken into account is obtained from integration of eqs. (28) and (29).

We illustrate this more general case by an example with $A = 1$, $j = 2 \times 10^8 A/m^2$, $\bar{s} = 10^{-4} m$, $\beta = 0.5$, $T_i(z_a) = 5 \times 10^4 K$, $T_e(z_a) = 10^6 K$, $T_e(z_a + L) = 5 \times 10^4 K$, and $z_a \ll L$. Here the plasma column can be divided into two regions:

(i) Within the region being close to the anode, the boundary conditions at $z = z_a$ and the finite value of the ion current result in a large difference between the ion and electron temperatures, as shown by Fig.5. The large corresponding temperature gradients in this region lead to a rapid decrease of $(T_e - T_i)/(T_e + T_i)$ down to a few percent, already at axial distances exceeding some $10^{-4} m$. This behaviour should only be considered as a formal solution of eqs. (28) and (29) which becomes modified in several ways near the anode. Thus, the finite Larmor radii tend to broaden this region and reduce its temperature gradients. Further, the presence of neutral gas at the anode reduces both the ion and electron temperatures and affects their gradients as outlined in Section 5.3.

(ii) At distances from the anode exceeding some $10^{-3} m$ the solution of eqs. (28) and (29) becomes as demonstrated by Fig.6, where the axial length $L = 0.129 m$ corresponds to the adopted boundary values of T_i and T_e. This solution deviates by less than 4 percent from the result obtained from expressions (36) and (37) which lead to $T_i = T_e = 0.74 \times 10^6 K$ close to the anode, i.e. at $z = z_a$.

5.3. The Temperature Gradient in the Electrode Layers

The heat balance conditions in the partially ionized anode layer are roughly given by eq. (40). From an earlier analysis of the plasma-neutral gas balance in a wall layer [18], the ratio between the ion and neutral particle densities near a wall surface is found to be of the order of $(T_n/T_i)^{1/2}$, at a local neutral gas temperature T_n. Further, the deduced layer thickness becomes quite small, i.e. of the order of $d_w = kT_i/2\pi m_i)^{1/2}/n\bar{s}$.

We shall not enter into a detailed discussion of the complicated balance in the anode layer, but only illustrate eq. (40) by an example with $A = 1$, $j = 2 \times 10^8 A/m^2$, $T = 5 \times 10^4 K$, $\xi = \xi_{max} = 10^{-14} m^3/s$, and $n = n_{na} = 10^{23} m^{-3}$. Then $dT/dz \approx 10^{10}[\exp(-2 \times 10^4 z) - 8 \times 10^{-3}]$ K/m. Lower values of T are likely to occur close to the anode surface, leading to a smaller effective cross-section σ_{ef} and a larger penetration length of the neutral gas, with a corresponding effect on dT/dz. In any case, these data indicate that there can exist a narrow partially ionized region near the anode surface within which a steep increase in the ion and electron temperatures takes place in the positive z direction.

6. Comments on Stability

Straight configurations of the present type have several stability features in common with their ring-shaped correspondence, with the exception of toroidal effects such as those being due to the plasma loop force. Part of the stability problems in Extrap systems have been investigated earlier [1-3, 15-17]. Here we shall only touch upon some questions concerning MHD stability:

(i) In both the unperturbed and perturbed states of a real plasma, the current density has to remain finite both at the boundary and in the interior of the plasma body. In other words, states or modes leading to excessively high current densities within thin plasma layers would become modified and damped by the large corresponding ohmic dissipation. A further constraint is imposed on the system in cases where the plasma temperature and the current density tend to zero at the plasma boundary.

(ii) Among the energy changes of possible perturbations in Extrap geometry, there arise several interdependent contributions, partly having opposite signs. Thus, the magnetic energy changes due to kinking become coupled with energy changes due to deformations of the non-circular plasma cross section, as well as with those being due to the displacements of the plasma in the inhomogeneous vacuum field which is being "anchored" in the external solid conductors. The released energy from kinking is related to the curvature of the bends of the plasma column, the energy changes from cross-section deformations arise from redistributions of the pinch force, and the changes due to the coupling with the vacuum field are related to the spatial gradients of the latter. Especially when the vacuum field has a zero at the axis, such as in Fig.1, its influence on stability is expected to become enhanced at decreasing distances between the outer plasma boundary and the external conductors.

(iii) The dependence of stability on the number of external conductors has to be further investigated. With a zero line of the vacuum field at the axis, the inhomogeneity of the field increases at a decreasing number of conductors. On the other hand, the conditions for ballooning instabilities to arise in the spacings between the conductors are expected to be favoured at a decreasing number of external conductors.

(iv) In the case of straight geometry, a "hardcore" conductor may be introduced at the axis, thereby adding a vacuum field component to a configuration where the plasma becomes confined in an annular region. By such an arrangement the stability of the conventional hardcore pinch could become improved by the external conductors. When the hardcore current is chosen in the opposite direction of the plasma current, part of the magnetic field from the latter is cancelled within the confinement region. Possibly this should allow for stronger plasma currents under controlled conditions than what would be the case in absence of a hardcore.

(v) Even limited periods of controllable and stable plasma conditions can be of considerable interest, provided that their duration is long enough for high plasma temperatures to be achieved.

7. Conclusions

Provided that a stable state with a clean plasma can be achieved during sufficiently long time intervals, linear schemes with a plasma column confined in a purely transverse magnetic field should provide an interesting alternative for achieving high plasma temperatures. From the results of this paper the following conclusions can be drawn:

(i) In the case of a purely transverse field there is a reduced transport of particles and heat to the ends of linear configurations, thus allowing for axial temperature gradients. These configurations could provide an alternative to open bottles such as mirror devices.

(ii) The present straight configurations have larger losses than closed toroidal schemes, but may still provide a line of interest to fusion research. As compared to a number of toroidal schemes, they also have advantages with respect to the possibilities of steady operation at high power inputs and beta values, to the absence of toroidal curvature effects, and to technical simplicity.

(iii) High plasma temperatures could be reached in linear geometry at technically feasible column lengths, even by means of ohmic heating. In devices of moderately large dimensions and technically realistic parameter values, thermonuclear ignition also appears to become possible. Whether reactor schemes based on these straight configurations become feasible is still an open question, partly due to the problems of stability, the large wall load of the present parameter ranges, and of plasma-wall interaction at the end electrodes.

8. Acknowledgements

The author is indebted to Drs. T. Hellsten and E. Tennfors for valuable discussions. Also the help with the numerical calculations of Section 5.2.2 by Mr. S. Holmberg and Dr. B. Bonnevier is gratefully acknowledged.

This work has been financially supported by the European Communities under an association contract between Euratom and Sweden.

Stockholm, August 14, 1978

9. References

[1] Lehnert, B., Royal Institute of Technology, Stockholm, TRITA-EPP-74-08(1974); Physica Scripta 10,139(1974).

[2] Hellsten, T., Royal Institute of Technology, Stockholm, TRITA-EPP-74-23(1974).

[3] Lehnert, B., Physica Scripta 16,147(1977).

[4] Bergström, J., Ekman, R., Hellsten, T., Lehnert, B., and Tennfors, E., unpublished work(1976).

[5] Drake, J. and Lehnert, B., unpublished work (1978).

[6] Lehnert, B., Physica Scripta 13,250(1976).

[7] Klüber, O., Z. Naturforschung 22a,1599(1967).

[8] Verboom, G.K., Plasma Physics 11,903(1969).

[9] Markvoort, J.A., FOM-Instituut voor Plasma-Fysica, Rijnhuizen Reports 75-90 and 75-91(1975).

[10] Kaufman, A.N., in Plasma Physics in Theory and Application (Ed. by W.B. Kunkel), McGraw-Hill Book Comp., New York(1966), Ch.4.

[11] Spitzer, L., Physics of Fully Ionized Gases, Interscience Publ., New York(1962).

[12] Ribe, F,L., Rev.Mod.Phys. 47,7(1975).

[13] Rose, D.J. and Clark, M., Plasmas and Controlled Fusion, MIT Press and Wiley (1961),Ch.11.

[14] Lehnert, B., Physica Scripta, 12,327(1975).

[15] Hellsten, T., Physica Scripta 13,313(1976).

[16] Hellsten, T., Royal Institute of Technology, Stockholm, TRITA-EPP-75-01(1975).

[17] Ring, R., Thesis, Uppsala University, Dept. of Theoretical Electrotechnics, Institute of Technology, Rep. UPTEC 7720 R, April (1977).

[18] Lehnert, B., Arkiv f. Fysik 28,499(1968).

Figure Captions

Fig.1. Outline of a straight Extrap configuration in which a plasma column within the shaded area is confined by a magnetic field $\underline{B}$ originating partly from the currents J_o in four rod-shaped external conductors, partly from the antiparallel plasma current density $\underline{j}$ being continuously distributed over the plasma body. The configuration is assumed to have a finite but comparatively large length in the axial z direction, with the plasma parameters varying rapidly with (x,y) in the transverse direction, and slowly with z.

Fig.2. The characteristic temperature T_η of ohmic heating given by eq. (37) as a function of the product $L \cdot j$ between the column length L and the current density j.

Fig.3. The maximum temperature $T(z_a)$ as a function of the effective length L of a plasma column with $J = 2.5 \times 10^6$A, $\beta = 0.5$, $A = 2.5$, and $\bar{a} = 10^{-2}$m. Full curve represents the balance in presence of alpha particle heating and broken line the case in absence of such heating. Alpha particles contained.

Fig.4. The relation between T_i and T_e when the ion current is neglected, $\bar{a} = 10^{-2}$m, and $\beta = 0.5$:

(a) $A = 1$ and $J = 6 \times 10^4$A.

(b) $A = 2.5$ and $J = 2 \times 10^6$A. Alpha particles contained.

Fig.5. Formal solution of the axial temperature profiles of ions and electrons near the pinch axis, in a region being close to the anode and with $A = 1$, $j = 2 \times 10^8$A/m^2, $\bar{a} = 10^{-2}$m, $\beta = 0.5$.

Fig.6. Same data as in Fig.5 but showing the axial temperature profiles along the entire plasma column.

Fig. 1

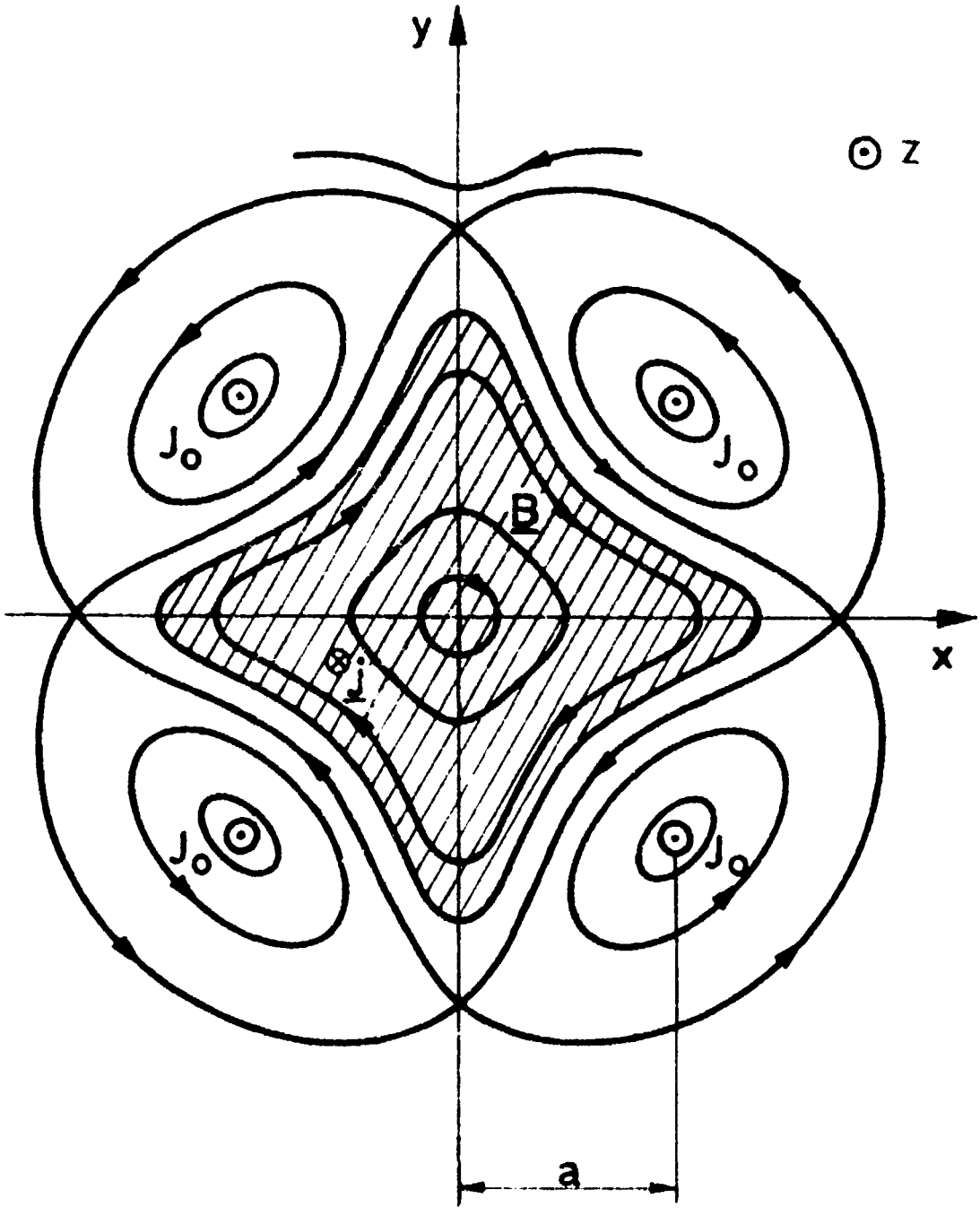

Fig. 2

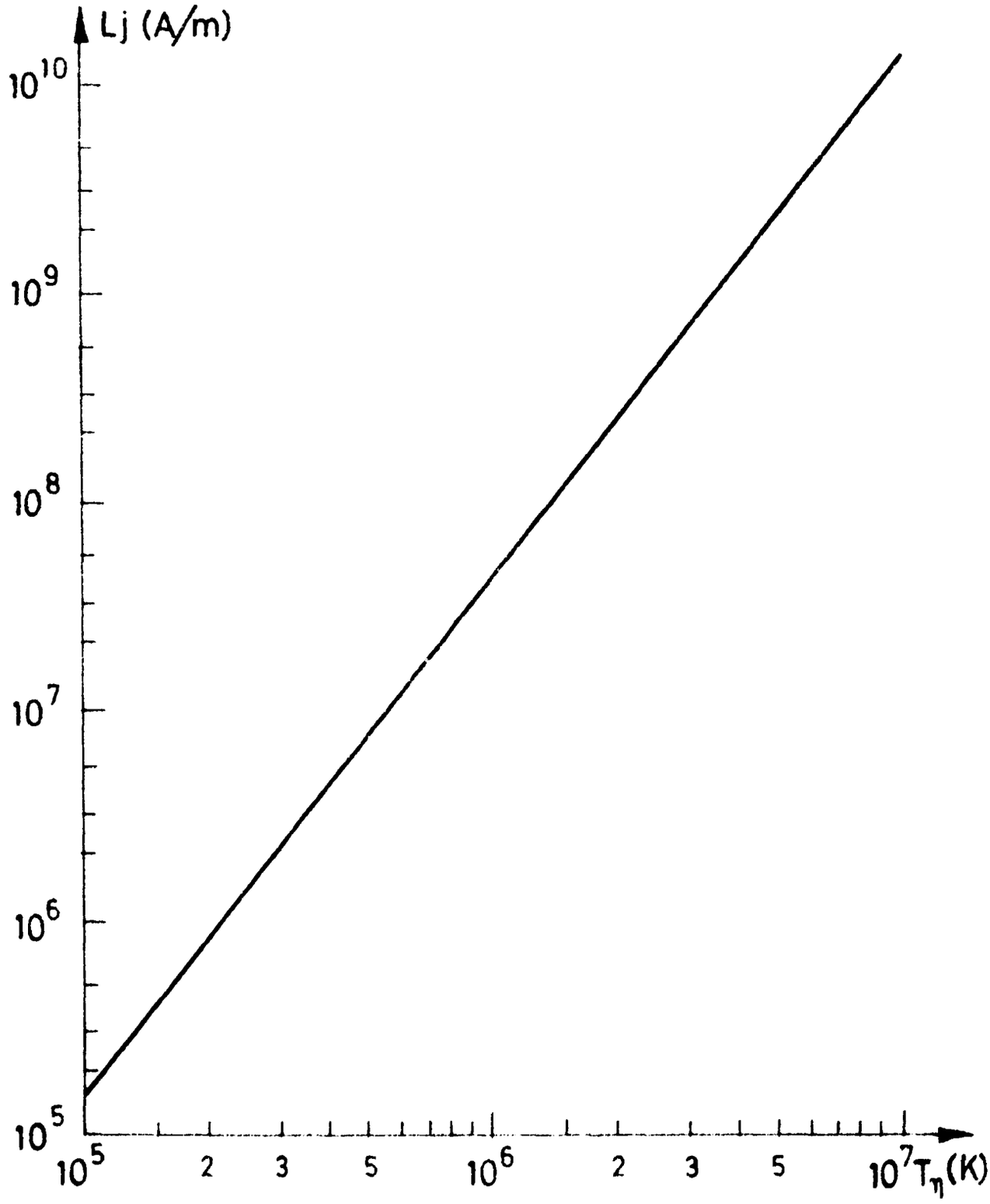

Fig. 3

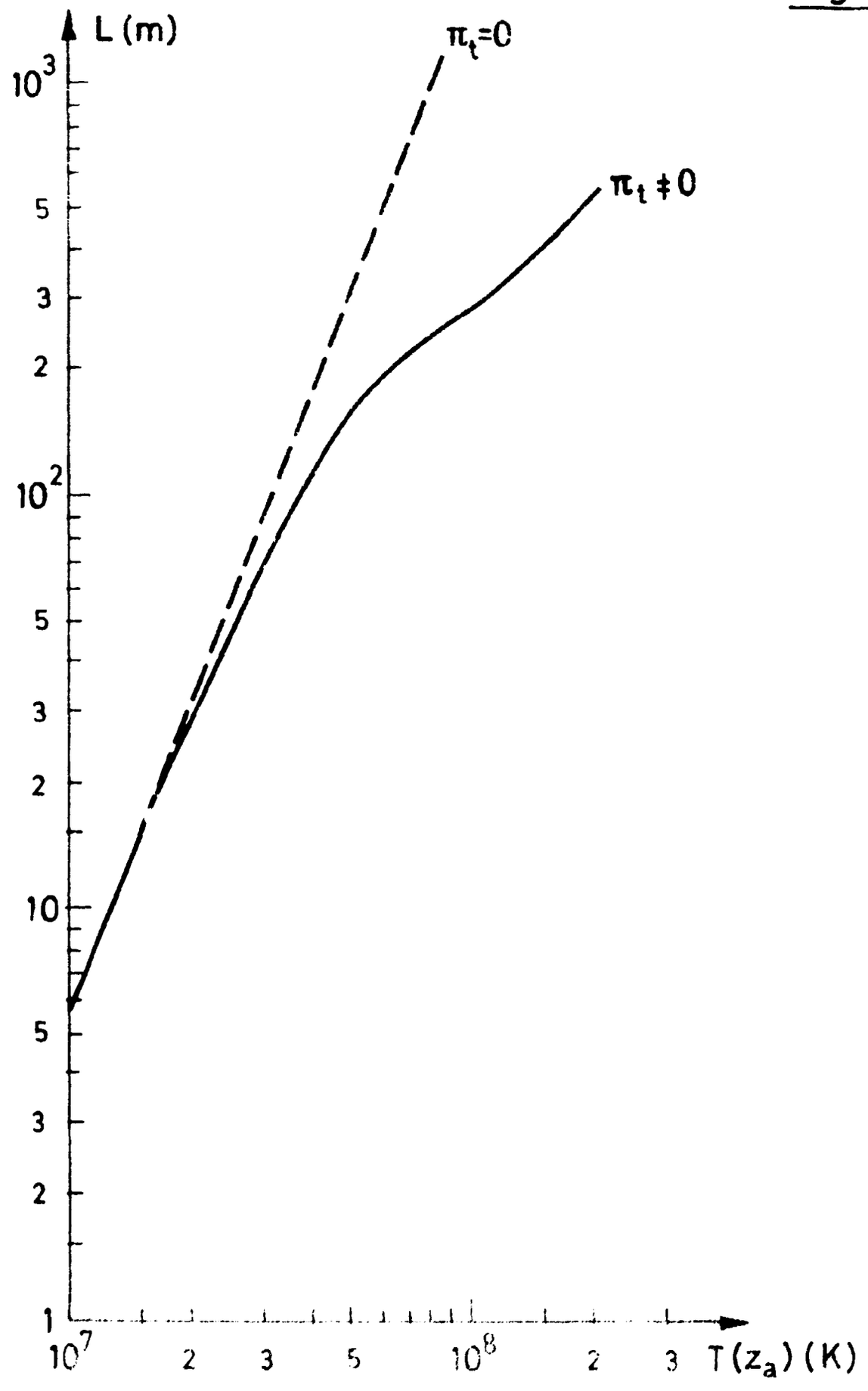

Fig. 4

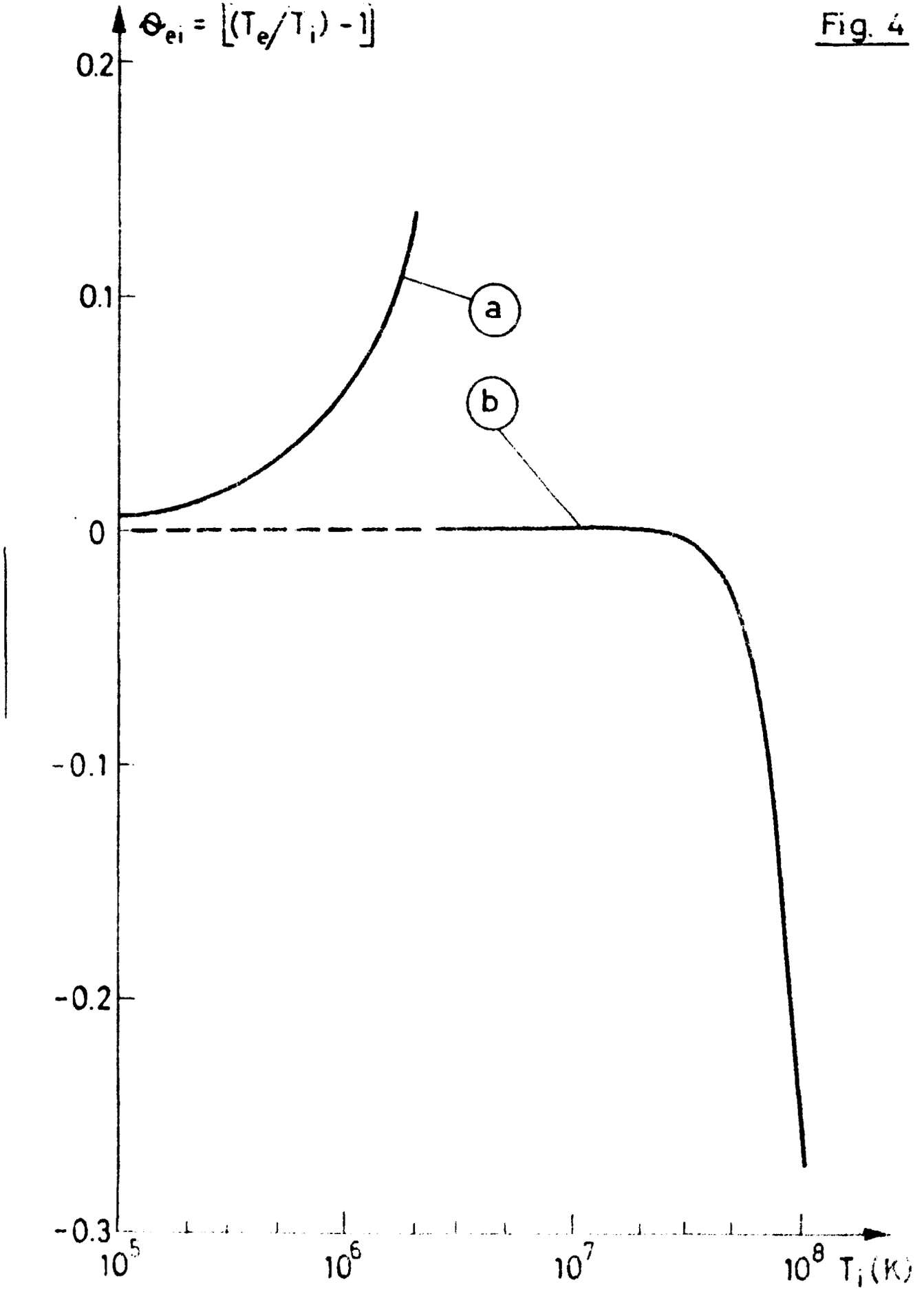

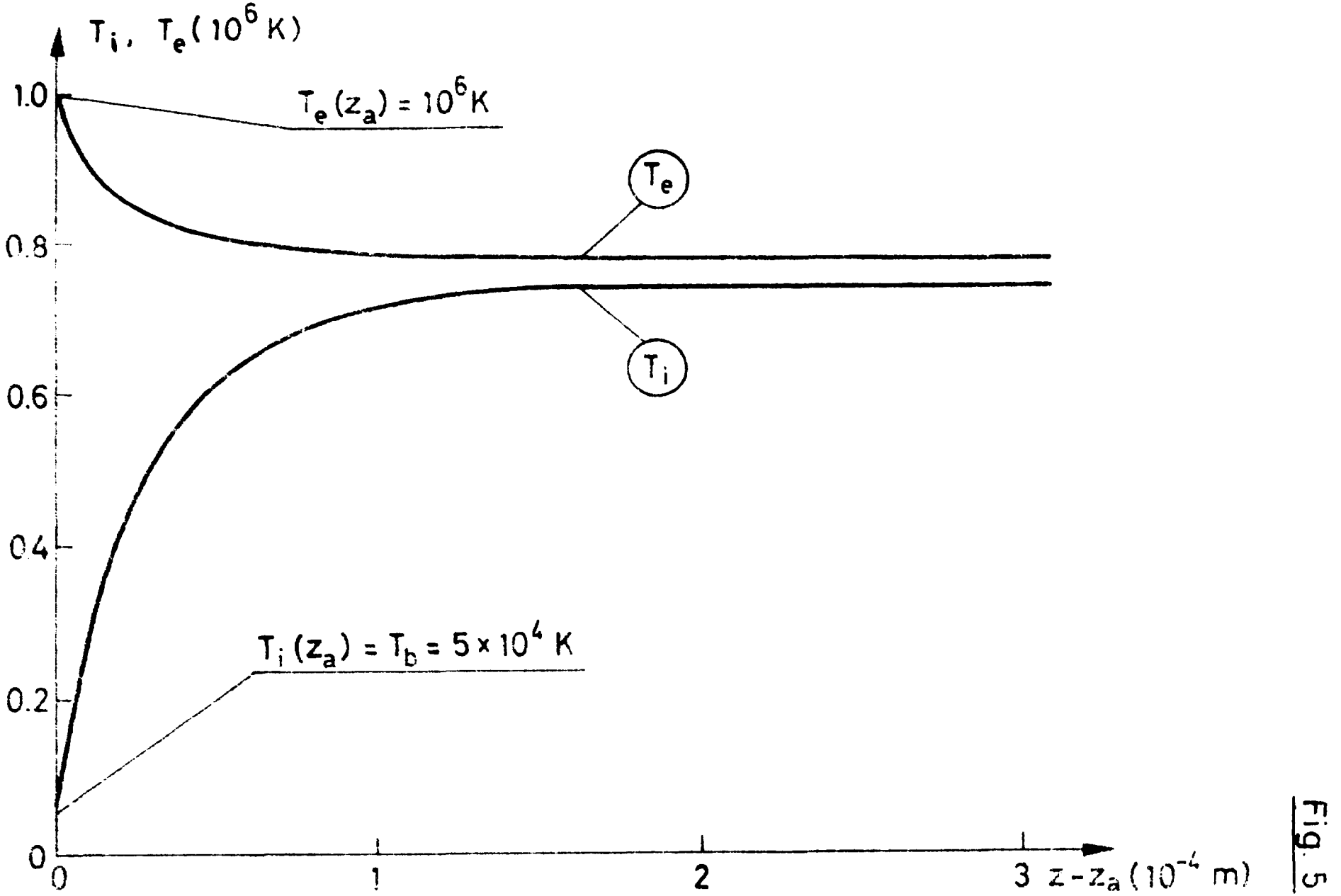
T_i, T_e (10^6 K)
1.0
0.8
0.6
0.4
0.2
0
$T_e(z_a) = 10^6$ K
T_e
T_i
$T_i(z_a) = T_b = 5 \times 10^4$ K
0
1
2
3 $z - z_a$ (10^{-4} m)

Fig. 5

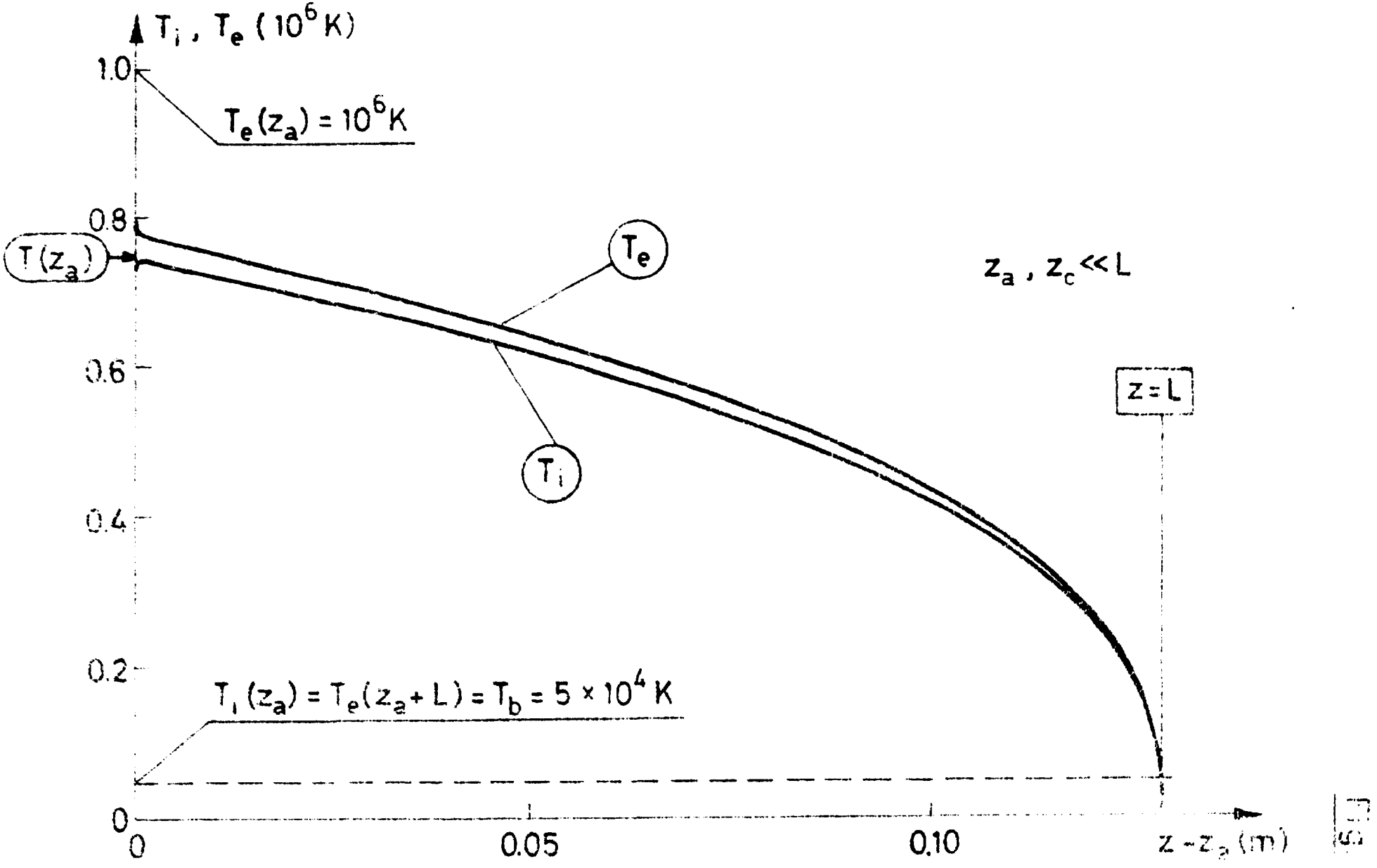
T_i , T_e (10^6 K)
1.0
$T_e(z_a) = 10^6$ K
0.8
$T(z_a)$
T_e
z_a , $z_c \ll L$
0.6
$z = L$
T_i
0.4
0.2
$T_i(z_a) = T_e(z_a + L) = T_b = 5 \times 10^4$ K
0
0
0.05
0.10
$z - z_a$ (m)

TRITA-PFU-78-06

Royal Institute of Technology, Department of Plasma Physics and Fusion Research, Stockholm, Sweden

ON THE BALANCE OF A LINEAR PLASMA COLUMN CONFINED IN A TRANSVERSE MAGNETIC FIELD

B. Lehnert, August 1978, 31 p. in English

The equilibrium features are investigated of a straight plasma column being confined in a purely transverse magnetic field, part of which is being generated by external conductors. Provided that stability can be secured at high beta values, the reduced transport of particles and heat in the axial direction should allow for large axial temperature gradients. It is then expected that temperatures even leading to ignition can be achieved in a pure plasma, at technically realistic column lengths.

Key words: Magnetic confinement, pinch, external conductors.